6

Main Dimensions of a Rotating Machine

In the previous chapters, the general theory governing the design of an electrical machine was presented: Chapter 1 addressed the necessary fundamentals of electromagnetic theory and Chapter 2 concentrated on winding arrangements. Chapter 3 described the behaviour of the magnetic circuit. Chapter 4 discussed the flux leakage and, finally, Chapter 5 focused on the resistances of the windings. We should now be able to commence the discussion of the main dimensions of electrical machine. The design of a rotating electrical machine can be commenced by defining certain basic characteristics, the most important of which are:

- Machine type (synchronous, asynchronous, DC, reluctance machine, etc.).
- Type of construction (external pole, internal pole, axial flux, radial flux machine, etc.).
- Rated power:
  - For electric motors, the shaft output power P_N in W is given.
  - For synchronous motors, also the power factor ($\cos\varphi$ overexcited) is given.
  - For induction and DC generators, the electric output power P_N in W is given. Induction generators take reactive power from the network according to their power factor. The reactive power must usually be compensated by capacitor banks.
  - For synchronous generators, the apparent power S_N is given in VA. The power factor (typically $\cos\varphi = 0.8$ overexcited) is also given.
- Rated rotational speed n_N of the machine or rated angular speed Ω_N.
- Number of pole pairs p of the machine (with frequency converter drives, this is also a subject of optimization).
- Rated frequency f_N of the machine (with frequency converter drives this is also a subject of optimization).
- Rated voltage U_N of the machine.
- Number of phases m of the machine.
- Intended duty cycle (S1–S9).
- Enclosure class and structure of the machine.

Design of Rotating Electrical Machines Juha Pyrhönen, Tapani Jokinen and Valéria Hrabovcová
 ISBN: 978-0-470-69516-6

- Additional information, such as efficiency, required locked rotor torque, pull-up torque, peak torque, locked rotor current, speed-controlled drive etc.
- Standards applied in the machine design.
- Economic boundary conditions.
- Manufacturability.

In machine design, there are a considerable number of free parameters. When aiming for an optimal solution, the task becomes extremely complicated unless the number of these free parameters is somehow limited. Many free parameters vary only slightly, and therefore, to simplify the task, these parameters can be assumed constant. The following 10 parameters can be selected as free parameters:

- outer diameter of the stator stack (with the standard IEC frames, this parameter is often fixed to certain values);
- length of the stator stack;
- width of the stator slot;
- height of the stator slot;
- diameter of the air gap;
- air-gap length;
- peak value of the air-gap flux density;
- width of the rotor slot;
- height of the rotor slot;
- pole pair number and frequency.

Actual machine design starts with the selection of the main dimensions of the machine. The term 'main dimensions' refers to the air-gap diameter D_s measured at the stator bore (see Figures 3.1 and 3.2) and the equivalent core length l' (see Figure 3.10 and Equation 3.36). The equivalent length of the core takes into account the influence of the flux fringing at possible cooling ducts of the machine and also at the ends of the machine.

In electrical machine design, there are certain empirically defined variation ranges of current and flux densities, which can be applied in the preliminary phase of the design. Tables 6.1 and 6.2 introduce some values of electromagnetic loadings for well-designed standard electrical machines.

The permitted loading levels are defined for a machine on the basis of the design of the insulation and the cooling of the machine. The values in the tables give some empirical information related to the selection of machine parameters. In principle, machine design is a rather complicated iteration process, in which the initial values are first selected for the dimensions of the machine. Next, the machine is designed electrically, and finally the cooling of the machine is computed. If the cooling of the machine is not efficient enough, the design has to be started from the beginning again by increasing the dimensions of the machine, by using better materials or by selecting a more efficient cooling method. The material selection has a significant influence on both the losses and the thermal resistances. If a low-loss iron material and high-thermal-class insulation materials are selected, the output power of the machine can be improved without increasing its size.

For permanent magnet machines, because of the limited remanence and coersivity of present-day magnets, we may select values in the lower half of the varying range according to Table 6.1 for synchronous machines.

Table 6.1 Permitted flux densities of the magnetic circuit for various standard electrical machines

	Flux density B/T			
	Asynchronous machines	Salient-pole synchronous machines	Nonsalient-pole synchronous machines	DC machines
Air gap	0.7–0.90 ($\hat{B}_{\delta 1}$)	0.85–1.05 ($\hat{B}_{\delta 1}$)	0.8–1.05 ($\hat{B}_{\delta 1}$)	0.6–1.1 (B_{max})
Stator yoke	1.4–1.7 (2)	1.0–1.5	1.1–1.5	1.1–1.5
Tooth (apparent maximum value)	1.4–2.1 (stator) 1.5–2.2 (rotor)	1.6–2.0	1.5–2.0	1.6–2.0 (compensating winding) 1.8–2.2 (armature winding)
Rotor yoke	1–1.6 (1.9)	1.0–1.5	1.3–1.6	1.0–1.5
Pole core	—	1.3–1.8	1.1–1.7	1.2–1.7
Commutating poles	—	—	—	1.3

When investigating the values of Table 6.2, it is worth noticing that when the dimensions of a slot are increased, lower values usually have to be selected than in the case of small slots. Hence, the lower values of J are for larger machines, and the highest values of J are suitable for small machines. Despite this, the lower values of A are valid for smaller machines and the higher ones for larger machines. If we are constructing PMSM fractional slot windings from small fractions with wide slots, the applicable values given in the table for pole windings are valid also in this case.

Table 6.2 Permitted RMS values for current densities J and linear current densities A for various electrical machines. Depending on the size of a permanent magnet machine, a synchronous machine, an asynchronous machine or a DC machine, suitably selected values can be used. Copper windings are generally assumed

			Nonsalient-pole synchronous machines			
			Indirect cooling			
	Asynchronous machines	Sailent-pole synchronous machines or PMSMs	Air	Hydrogen	Direct water cooling	DC machines
A/kA/m	30–65	35–65	30–80	90–110	150–200	25–65
	Stator winding	Armature winding		Armature winding		Armature winding
J/A/mm^2	3–8	4–6.5	3–5	4–6	7–10	4–9
	Copper rotor winding	Field winding:				Pole winding
J/A/mm^2	3–8	2–3.5				2–5.5
	Aluminium rotor winding	Multi-layer		Field winding		Compensating winding
J/A/mm^2	3–6.5	2–4	3–5	3–5	6–12	3–4
		Single-layer	With direct water cooling, in field windings 13–18 A/mm^2 and 250–300 kA/m can be reached			

Table 6.3 Tangential stresses $\sigma_{F\tan}$ calculated from the values of Tables 6.1 and 6.2. There are three stress values, calculated with the lowest linear current density and flux density, with the average values and with the highest values. The flux density and linear current density distributions are assumed sinusoidal. For DC machines, a pole width coefficient of 2/3 is assumed. The power factor of synchronous machines is assumed to be 1, and for asynchronous machines, 0.8

	Totally enclosed asynchronous machines	Sailent-pole synchronous machines or PMSMs	Nonsalient-pole synchronous machines				
			Indirect cooling		Direct water cooling	DC machines
			Air	Hydrogen		
A/kA/m, RMS	30–65	35–65	30–80	90–110	150–200	25–65
Air-gap flux density $\hat{B}_{\delta 1}$/T	0.7–0.9	0.85–1.05	0.8–1.05	0.8–1.05	0.8–1.05	0.6–1.1
Tangential stress $\sigma_{F\tan}$/Pa						
minimum	12 000*	21 000*	17 000*	51 000*	85 000*	12 000*
average	21 500*	33 500*	36 000*	65 500*	1,14 500*	29 000*
maximum	33 000*	48 000*	59 500*	81 500*	1,48 500*	47 500*
	*$\cos\varphi = 0.8$	*$\cos\varphi = 1$	*$\cos\varphi = 1$	*$\cos\varphi = 1$	*$\cos\varphi = 1$	*$\alpha_{\mathrm{DC}} = 2/3$

In Equation (1.115) we defined the tangential stress $\sigma_{F\tan}$ in the air gap. The local value for the tangential stress depends on the local linear current density $A(x)$ and the local flux density $B(x)$, $\sigma_{F\tan}(x) = A(x)B(x)$. If a sinusoidal air-gap flux density with peak value $\hat{B}_\delta$ is assumed, and a sinusoidal linear current density with peak value $\hat{A}$ and RMS value A is applied, we obtain for the average tangential stress

$$\sigma_{F\tan} = \frac{\hat{A}\hat{B}_\delta \cos\varphi}{2} = \frac{A\hat{B}_\delta \cos\varphi}{\sqrt{2}}. \tag{6.1}$$

This tangential stress produces the torque of the machine when acting upon the rotor surface. Table 6.3 illustrates the guiding limit values for the tangential stress of the air gap calculated from Tables 6.1 and 6.2.

Typical tangential stress values give us a starting point for the design of an electrical machine. We may define the size of the rotor first by using a suitable tangential stress value on the rotor surface. If the rotor radius is r_r, the rotor equivalent length is l', the rotor surface facing the air gap is S_r, and the average tangential stress on the surface is $\sigma_{F\tan}$, we may write the torque T of the rotor simply as

$$\begin{aligned} T &= \sigma_{F\tan} r_\mathrm{r} S_\mathrm{r} \\ &= \sigma_{F\tan} r_\mathrm{r}\left(2\pi r_\mathrm{r} l'\right) \\ &= \sigma_{F\tan} 2\pi r_\mathrm{r}^2 l' \\ &= \sigma_{F\tan} \pi \frac{D_\mathrm{r}^2}{2} l' = 2\sigma_{F\tan} V_\mathrm{r}. \end{aligned} \tag{6.2}$$

The correct rotor volume V_r to produce a certain torque can easily be estimated with Equation (6.2).

A similar basis for the design of the machine rotor size is the machine constant C of a well-designed electrical machine. The machine constant C expresses the magnitude of the 'internal' apparent power S_i or the power P_i given by the rotor volume of the machine. By employing the emf E_m induced over the magnetizing inductance L_m of the phase (the emf is calculated from the peak value $\hat{\Psi}_m$ of the air-gap flux linkage in one phase, see Equation 7.3) and the current I_s of the stator phase, we obtain the apparent power S_i for rotating-field machines rotating at a synchronous speed $n_{syn} = f/p$

$$S_i = mE_m I_s. \tag{6.3}$$

The air-gap emf E_m can be substituted into Equation (6.3), and we obtain

$$S_i = m\frac{1}{\sqrt{2}}\omega\hat{\Psi}_m I_s = m\frac{1}{\sqrt{2}}\omega N_s k_{ws1}\hat{\Phi}_m I_s. \tag{6.4}$$

The maximum flux $\hat{\Phi}_m$ penetrating a phase winding will be found by integrating the air-gap flux density $B_\delta(x)$ over the pole surface S_p

$$\hat{\Phi}_m = \int_{S_p} B_\delta \, dS_p. \tag{6.5}$$

If the air-gap flux density has a sinusoidal distribution over the pole pitch τ_p and there is no variation with respect to the length of the machine l', the surface integral can be simplified as

$$\begin{aligned}\hat{\Phi}_m &= \int_0^{\tau_p} l' \cdot \hat{B}_\delta \sin\frac{x\pi}{\tau_p}\, dx \\ &= l'\tau_p \alpha \hat{B}_\delta.\end{aligned} \tag{6.6}$$

The product $\alpha\hat{B}_\delta$ represents the average value of the flux density in the air gap. In the case of a sinusoidal distribution $\alpha = 2/\pi$. In other cases, a suitable value for α has to be found by integrating the flux density over the pole surface. For instance, if we have surface magnets on the rotor, the air-gap flux density created by the permanent magnets is usually nonsinusoidal. In such a case, the average value α for the flux density in the air gap can be defined from the relative magnet width α_{PM}.

The RMS value of the linear current density A of the stator may be defined from the stator slot pitch τ_s and the RMS value of slot current I_u (assuming that there are no parallel paths in the winding and the winding is a full-pitch one, $I_u = I_s z_Q$). The number of slots in the stator is Q_s. Thus

$$A = \frac{I_u}{\tau_s}, \tag{6.7}$$

$$\tau_s = \frac{\pi D}{Q_s}. \tag{6.8}$$

Here D is, for generality, used instead of the stator inner or rotor outer diameter ($D \approx D_r \approx D_s$).

The number of conductors in the slot z_{Q} with all turns in series is

$$z_{\mathrm{Q}} = \frac{N_{\mathrm{s}}}{pq} = \frac{N_{\mathrm{s}}}{p\dfrac{Q_{\mathrm{s}}}{2pm}} = \frac{2N_{\mathrm{s}}m}{Q_{\mathrm{s}}}. \tag{6.9}$$

Now we may write for the linear current density

$$A = \frac{I_{\mathrm{u}}}{\tau_{\mathrm{s}}} = \frac{I_{\mathrm{u}}Q_{\mathrm{s}}}{\pi D} = \frac{I_{\mathrm{s}}z_{\mathrm{Q}}Q_{\mathrm{s}}}{\pi D} = \frac{2I_{\mathrm{s}}N_{\mathrm{s}}m}{\pi D}. \tag{6.10}$$

We solve the above for I_{s} and substitute I_{s} into Equation (6.4)

$$S_{\mathrm{i}} = m\frac{1}{\sqrt{2}}\omega N_{\mathrm{s}}k_{\mathrm{w1}}\hat{\Phi}_{\mathrm{m}}I_{\mathrm{s}} = m\frac{1}{\sqrt{2}}\omega N_{\mathrm{s}}k_{\mathrm{ws1}}\hat{\Phi}_{\mathrm{m}}\frac{A\pi D}{2N_{\mathrm{s}}m} = \frac{1}{\sqrt{2}}\omega k_{\mathrm{ws1}}\hat{\Phi}_{\mathrm{m}}\frac{A\pi D}{2}. \tag{6.11}$$

We now substitute $\omega = 2p\pi n_{\mathrm{syn}}$ and the peak flux from Equation (6.6) into Equation (6.11)

$$\begin{aligned} S_i &= \frac{1}{\sqrt{2}}2p\pi n_{\mathrm{syn}}k_{\mathrm{ws1}}\frac{2}{\pi}\frac{\pi D}{2p}\hat{B}_{\delta}l'\frac{A\pi D}{2} \\ &= \frac{\pi^2}{\sqrt{2}}n_{\mathrm{syn}}k_{\mathrm{ws1}}A\hat{B}_{\delta}l'D^2. \end{aligned} \tag{6.12}$$

We may now rewrite this as

$$\begin{aligned} S_{\mathrm{i}} &= mE_{\mathrm{m}}I_{\mathrm{s}} = \frac{\pi^2}{\sqrt{2}}k_{\mathrm{ws1}}A\hat{B}_{\delta}D^2l'n_{\mathrm{syn}} \\ &= CD^2l'n_{\mathrm{syn}}. \end{aligned} \tag{6.13}$$

The machine constant C can be written in the following form for rotating-field machines (synchronous and asynchronous machines), according to Equation (6.13):

$$C = \frac{\pi^2}{\sqrt{2}}k_{\mathrm{w1}}A\hat{B}_{\mathrm{m}} = \frac{\pi^2}{2}k_{\mathrm{ws1}}\hat{A}\hat{B}_{\delta}, \tag{6.14}$$

where $A = \hat{A}/\sqrt{2}$. l' is the equivalent length of the machine and A is the RMS value of the linear current density, which corresponds to the tangential magnetic field strength H_{tan} in the air gap, see Chapter 1.

The rotor volume V_{r} required for a certain apparent power can now be written as

$$V_{\mathrm{r}} = \frac{\pi}{4}D_{\mathrm{r}}^2l' = \frac{\pi}{4}\frac{S_{\mathrm{i}}}{Cn_{\mathrm{syn}}}. \tag{6.15}$$

The weight of the rotor is proportional to its volume

$$m_{\mathrm{r}} \sim V_{\mathrm{r}} = \frac{\pi}{4}\frac{pS_{\mathrm{i}}}{Cf}. \tag{6.16}$$

In DC machines, the air-gap flux density is not sinusoidal. Under the pole at no load, we have the air-gap flux density $B_{\max}$. For DC machines, the internal power of which is defined $P_{\mathrm{i}} = \pi^2 \alpha_{\mathrm{DC}} A B_{\delta\,\max} D^2 l' n_{\mathrm{syn}} = C D^2 l' n_0$, we may write

$$C = \pi^2 \alpha_{\mathrm{DC}} A B_{\delta\,\max}. \tag{6.17}$$

α_{DC} is the relative pole width coefficient for DC machines (typically about 2/3).

The dependence of the internal apparent power S_{i} on the mechanical power P_{mec} of a rotating-field machine is obtained from the power factor $\cos\varphi$ of the machine and the efficiency η (which have to be estimated at this stage). Now, the machine constant of mechanical power C_{mec} can be introduced:

$$P_{\mathrm{mec}} = \eta m U I \cos\varphi = \eta \cos\varphi \frac{U}{E} S_{\mathrm{i}} = C_{\mathrm{mec}} D^2 l' n_{\mathrm{syn}}. \tag{6.18}$$

In a DC machine, the internal power ($P_{\mathrm{i}} = E I_{\mathrm{a}}$) depends on the input power $P_{\mathrm{in}} = U_{\mathrm{a}} I_{\mathrm{a}}$; consequently, based on their ratio, we may write

$$P_{\mathrm{i}} = \frac{E}{U_{\mathrm{a}}} \frac{I_{\mathrm{a}}}{I_{\mathrm{a}}} P_{\mathrm{in}} \tag{6.19}$$

where I_{a} is the armature current.

With Equation (6.16) and Equation (6.14), we obtain for AC machines

$$m_{\mathrm{r}} \sim \frac{p S_{\mathrm{i}}}{f A \hat{B}_{\delta}} \sim \frac{p S_{\mathrm{i}}}{f \sigma_{F\,\tan}}. \tag{6.20}$$

Thus, the higher the tangential stress and the supply frequency, the lower the weight of the rotor.

By selecting a small number of pole pairs p and a high supply frequency f, we obtain, in principle, a light machine for a certain output power. Since the output power of a machine depends on the torque T and the mechanical angular frequency Ω, as $P = \Omega\, T$, the torque of a high-speed machine is small when compared with a low-speed machine of equal output power. At high speeds, however, the motor power density increases together with the loss density, and hence effective methods to reduce the losses and to improve the cooling of the machine have to be applied. With high frequencies, suitable means to reduce the stator winding skin effect have to be adopted so that there is no need to reduce greatly the linear current density. As the frequency rises, in order to maintain the air-gap flux density, better stator steel materials and more effective cooling methods have to be selected.

When analysing the weight of 22 kW serial-produced machines, we may construct a curve according to Figure 6.1 as a function of the number of pole pairs. The dotted line in the figure approximates the weight of the machine as a function of the number of pole pairs. We can see that, in principle, the weight of the machine follows the equation

$$m = m_0 + K p. \tag{6.21}$$

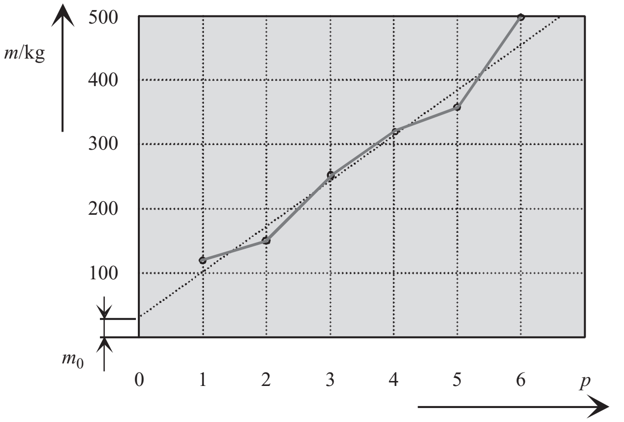

Figure 6.1 Weight of typical, totally enclosed, industrial 22 kW, 50 Hz, 400 V induction motors as a function of the number of pole pairs. In the figure $m_0 = 40\,\mathrm{kg}$

According to Equation (6.20), the weight of a machine is inversely proportional to the frequency, and thus the weight of the machine should be

$$m = m_0 + \frac{K}{f^{g}}, \tag{6.22}$$

where m_0, K and g are constants. Further, g is usually less than one, since the linear current density and the air-gap flux density cannot be considered constant as the frequency of the machine increases. As a result, we obtain Figure 6.2, which illustrates the approximate weight of a two-pole induction machine as a function of frequency f.

The allowed linear current densities and the air-gap flux densities of electrical machines are strongly dependent on the cooling methods, as shown in Tables 6.1 and 6.2. Highly effective cooling methods increase the permitted electromagnetic loadings 1.5–2-fold, and correspondingly the weight of the machine drops by 30–50%. In well-designed machines, the linear current density and the flux density depend on the machine size in such a way that they both increase as the size of the machine increases. As a result, the machine constant also depends on the size of the machine. Figure 6.3 illustrates the machine constant of induction and synchronous machines of different sizes per pole power. Because of the low excitation losses in permanent magnet machines, the machine constants for PMSMs could be high. The values given in the tables are, however, also limitedly valid for PMSMs, because the permanent magnet rotor temperature must be limited to lower values than in wound rotors or die-cast rotors, especially when NdFeB magnets are used. Typically, 100 °C should not be exceeded with NdFeB magnets to minimize the magnet demagnetization risk under the demagnetizing armature reaction. SmCo magnets tolerate high temperatures, but their remanence is remarkably lower than that of NdFeB magnets.

The machine constants of different machine types are not exactly equal. The definition of machine constants is based on empirical knowledge and the tradition of machine construction, and therefore even quite contradictory values for machine constants can be found in the literature. With a constant supply frequency, the rotor peripheral speed in rotating-field machines is proportional to the pole pitch. The permitted armature current and thereby the machine

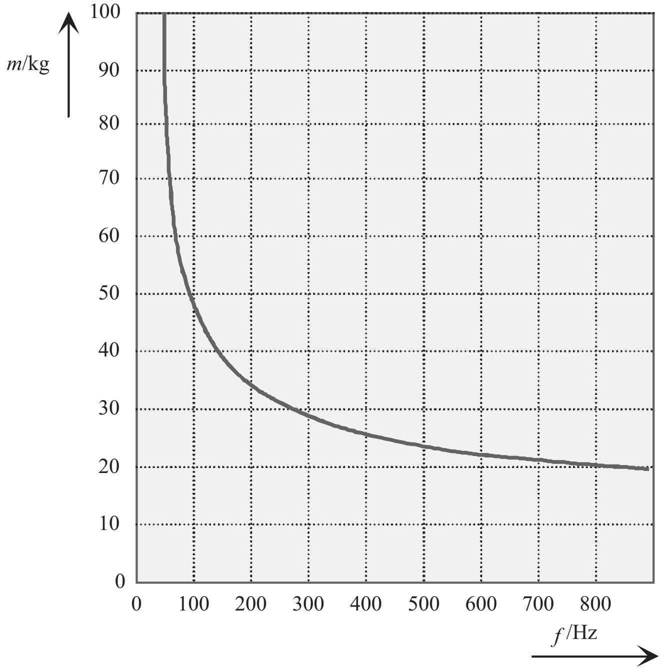

Figure 6.2 Weight of the active parts of a two-pole 22 kW induction motor as a function of frequency. The exponent $g \approx 0.8$ in Equation (6.22)

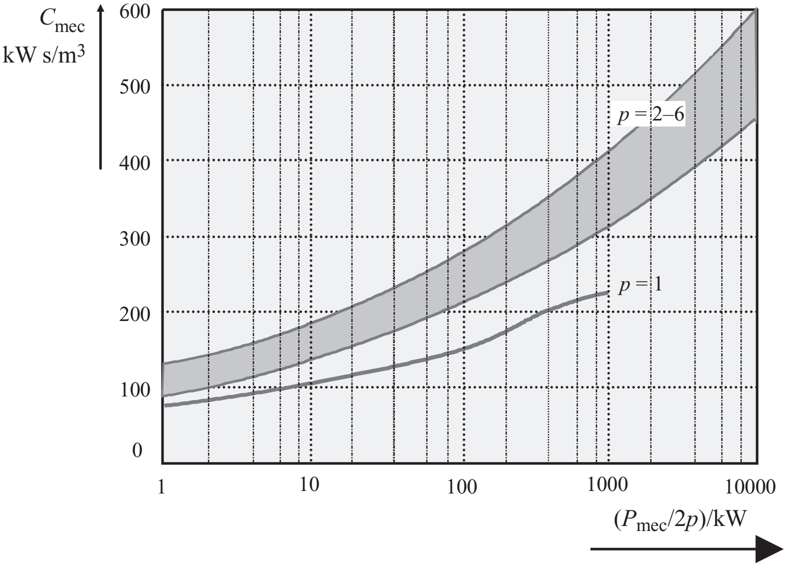

Figure 6.3 Machine constants of totally enclosed asynchronous and synchronous machines as a function of pole power

constant are functions of the pole pitch and the frequency of the machine. Since the pole pitch of a machine cannot be deduced from its rated values, the machine constant is often given as a function of pole power ($P_{mec}/2p$). The method can be justified by the fact that the ratio of the length and the pole pitch is fairly constant irrespective of the number of pole pairs.

Example 6.1: The diameter of a rotor of a 4 kW, 50 Hz, two-pole ($n_{syn} = 50$/s) induction motor is 98 mm and the length is 82 mm. Assume 1% rated slip and calculate the machine constant and the average tangential stress.

Solution: The rated torque of the motor is

$$T_N = \frac{P}{\Omega} = \frac{P}{(1-s)\Omega_{syn}} = \frac{4000\,\mathrm{W}}{(1-0.01)\cdot 2\pi \cdot 50/\mathrm{s}} = 12.86\,\mathrm{N\,m}.$$

The torque-producing area of the rotor is $S_r = \pi D_r l = 0.0252\,\mathrm{m}^2$. The radius of the rotor is 49 mm, and hence the tangential force at the rotor surface is on average

$$T_N = F_{tan} r_r \Leftrightarrow F_{tan} = \frac{T_N}{r_r} = \frac{12.86\,\mathrm{N\,m}}{0.049\,\mathrm{m}} = 262\,\mathrm{N}.$$

The average tangential stress is

$$\sigma_{F\,tan} = \frac{F_{tan}}{S_r} = \frac{262\,\mathrm{N}}{0.0252\,\mathrm{m}^2} = 10\,400\,\mathrm{N/m}^2.$$

The corresponding machine constant becomes

$$P_{mec} = C_{mec} D^2 l' n_{syn} \Leftrightarrow C_{mec} = \frac{P_{mec}}{n_{syn} D^2 l'} \approx \frac{4\,\mathrm{kW}}{50/\mathrm{s}\cdot(0.098\,\mathrm{m})^2\cdot 0.082\,\mathrm{m}} = 102\,\mathrm{kW\,s/m}^3.$$

The pole power of the machine is now 2 kW, and consequently this point is located somewhat higher than the curve of $p = 1$ in Figure 6.3.

Example 6.2: Repeat Example 6.1 for a 30 kW, 50 Hz, four-pole ($n_{syn} = 25$/s, 190 N m) induction motor. The rotor diameter is 200 mm and the rotor length 206 mm.

Solution: $T_N = 190\,\mathrm{N\,m}$.

$$F_{tan} = \frac{T_N}{r_r} = \frac{190\,\mathrm{N\,m}}{0.1\,\mathrm{m}} = 1900\,\mathrm{N}.$$

$$\sigma_{tan} = \frac{F_{tan}}{S_r} = \frac{1900\,\mathrm{N}}{\pi\cdot 0.2\,\mathrm{m}\cdot 0.206\,\mathrm{m}} = 14\,700\,\mathrm{N/m}^2.$$

The corresponding machine constant becomes

$$C_{\mathrm{mec}} = \frac{P_{\mathrm{mec}}}{n_{\mathrm{syn}} D^2 l'} \approx \frac{30\,\mathrm{kW}}{25/\mathrm{s} \cdot (0.2\,\mathrm{m})^2 \cdot 0.206\,\mathrm{m}} = 146\,\mathrm{kW\,s/m^3}.$$

The pole power of the machine is 7.5 kW, and this point is well within the region of $p = 2$–6 of Figure 6.3.

The machine constant of doubly salient reluctance machines can with low outputs be notably higher than the machine constant of an induction machine. For instance, according to Lawrenson (1992), the machine constants of an 11 kW DC machine, an induction machine and a doubly salient reluctance machine are in the ratio 1 : 1.23 : 1.74. Thus, in this power class, the machine constant of a doubly salient reluctance machine is about 40% higher than the machine constant of an induction motor. Although it was invented a long time ago, the doubly salient reluctance machine is still at the very beginning of its development. The machine was employed in the early twentieth century to aim the guns of British warships. Nowadays, the development of power electronics is bringing these machines into wider use.

6.1 Mechanical Loadability

In addition to temperature rise, the output power and maximum speed of a machine are restricted by the highest permissible mechanical stresses caused by the centrifugal force, natural frequencies and by the highest permissible electrical and magnetic loadings (see Sections 6.2 and 6.3).

The highest stress σ_{mec} caused by the centrifugal force in the rotor is proportional to the square of the angular speed

$$\sigma_{\mathrm{mec}} = C' \rho r_{\mathrm{r}}^2 \Omega^2. \tag{6.23}$$

Here

$C' = \frac{3+\nu}{8}$ for a smooth homogeneous cylinder,
$C' = \frac{3+\nu}{4}$ for a cylinder with a small bore,
$C' \approx 1$ for a thin cylinder,
r_{r} is the radius of the rotor,
Ω is the mechanical angular speed,
ρ is the density of the material,
ν is Poisson's ratio (i.e. the ratio of lateral contraction to longitudinal extension in the direction of the stretching force).

When the maximal mechanical stress of the rotor material is known, the equation can be used to determine the maximum allowable radius r of the rotor. Typically, a safety factor has to be used so as not to exceed the integrity of the rotor material.

Poisson's ratios vary slightly for different materials. Table 6.4 lists some ratios for pure materials.

Example 6.3: Calculate the maximum diameter for a smooth steel cylinder having a small bore. The cylinder is rotating at 15 000 min^{-1}. The yield strength for the material is 300 N/mm^2 = 300 MPa. The density of the steel is $\rho = 7860\,\mathrm{kg/m^3}$.

Solution: Poisson's ratio for steel is 0.29. For a cylinder with a small bore

$$C' = \frac{3+\nu}{4} = \frac{3+0.29}{4} = 0.823.$$

The stress is calculated as $\sigma_{\mathrm{mec}} = C'\rho r_{\mathrm{r}}^2 \Omega^2$

$$\sigma_{\mathrm{yield}} = C'\rho r_{\mathrm{r}}^2 \Omega^2 \Leftrightarrow r_{r,\max} = \sqrt{\frac{\sigma_{\mathrm{yield}}}{C'\rho\Omega^2}} = \sqrt{\frac{300\,\mathrm{MPa}}{0.823 \cdot 8760\,\mathrm{kg/m^3} \cdot \dfrac{(2 \cdot (15\,000/60) \cdot \pi)^2}{\mathrm{s}^2}}} = 0.13\,\mathrm{m}.$$

As there must be some security in the yield stress, the radius of the rotor diameter has to be smaller than what was calculated above.

Equation (6.23) cannot be directly applied to the measurement of stresses in rotor laminations, for instance, because of the fairly complicated geometry of the laminations. However, some informative results may be found, since the stress is always highest at the centre of a solid plate or at the inner surface of a plate with a centre bore. At these points, the permitted proportion of the yield stress of the material should not be exceeded.

In the case of salient-pole rotors, in small machines, the pole cores should be fastened to the shaft for instance using screws. The screw fastenings have to be dimensioned with a sufficient security depending on the yield stress. If a screw fastening is out of the question, a dovetail joint may be applied.

The maximum stress in a rotor caused by the centrifugal force is, according to Equation (6.23), proportional to the square of the peripheral speed. Thus, we can find fixed values for a maximum peripheral speed and stress. If the rotor dimensions (diameter, length, etc.) of the machine are assumed to be variable over the scale λ (lengths and diameters are proportional to λ, areas to λ^2 and volumes to λ^3), the maximum speed of the machine becomes inversely proportional to the scale λ:

$$n_{\max} \sim \lambda^{-1}. \tag{6.24}$$

Table 6.4 Poisson's ratios for certain pure metals

Metal		ν	Metal		ν
Aluminium	Al	0.34	Nickel	Ni	0.30
Copper	Cu	0.34	Titanium	Ti	0.34
Iron	Fe	0.29	Cobalt	Co	0.31

6.2 Electrical Loadability

Resistive losses P_{Cu} in a winding are proportional to the square of the current density J and to the mass of the conductors

$$P_{\mathrm{Cu}} \sim J^2 m_{\mathrm{Cu}} \sim J^2 \lambda^3. \tag{6.25}$$

The thermal resistance R_{th} between the conductors and the teeth is

$$R_{\mathrm{th}} = \frac{d_{\mathrm{i}}}{\lambda_{\mathrm{i}} S_{\mathrm{i}}}, \tag{6.26}$$

where d_{i} is the thickness of the slot insulation, λ_{i} the thermal conductivity of the insulation and S_{i} the area of the slot wall. The thickness of the insulation d_{i} is constant independent of the machine size (it depends on the rated voltage) and hence

$$R_{\mathrm{th}} \sim \frac{1}{\lambda^2}. \tag{6.27}$$

The temperature difference ΔT between the conductors and the teeth is

$$\Delta T = P_{\mathrm{Cu}} R_{\mathrm{th}} \sim J^2 \lambda. \tag{6.28}$$

Consequently, for a given temperature difference,

$$J^2 \lambda = \text{constant} \tag{6.29}$$

and

$$J \sim \frac{1}{\sqrt{\lambda}}. \tag{6.30}$$

Thus, small machines tolerate higher current densities better than large machines.

The linear current density A in this case may be calculated as the total RMS current in a slot $JS_{\mathrm{Cu,u}}$ divided by the slot pitch τ_{u}

$$A = \frac{JS_{\mathrm{Cu,u}}}{\tau_{\mathrm{u}}} \sim \frac{\frac{1}{\sqrt{\lambda}}\lambda^2}{\lambda} = \sqrt{\lambda}. \tag{6.31}$$

The linear current density A and the current density J are dimensions of the electrical loading of a machine. As the current density in small machines can be higher than in large machines, the linear current density behaves in the opposite sense: the linear current density is higher in large machines than in small machines. The product of A and J is

$$AJ \sim \sqrt{\lambda}\frac{1}{\sqrt{\lambda}} = 1 = \text{constant}, \tag{6.32}$$

and thus AJ is independent of the size of the machine; it depends only on the effectiveness of the cooling of the machine. For totally enclosed machines, AJ is smaller than for open-circuit cooling. In air-cooled machines, the product AJ ranges from $10 \times 10^{10}\,\mathrm{A^2/m^3}$ to $35 \times 10^{10}\,\mathrm{A^2/m^3}$, but in different machines with the same kind of cooling, the product is approximately the same independent of the machine size. In the case of direct water cooling, AJ attains essentially higher values.

Example 6.4: Using Table 6.2, calculate the AJ values for different machines.

Solution:

	Asynchronous machines	Sailent-pole synchronous machines or PMSMs	Nonsalient-pole synchronous machines: Indirect cooling: Air	Nonsalient-pole synchronous machines: Indirect cooling: Hydrogen	Nonsalient-pole synchronous machines: Direct water cooling	DC machines
A/kA/m	30–65	35–65	35–80	90–110	150–200	25–65
	Stator winding	Armature winding		Armature winding		Armature winding
$J/\mathrm{A/m^2}$	$3–8 \times 10^6$	$4–6.5 \times 10^6$	$3–5 \times 10^6$	$4–6 \times 10^6$	$7–10 \times 10^6$	$4–9 \times 10^6$
$AJ/\mathrm{A^2/m^3}$	9×10^{10} to 52×10^{10}	14×10^{10} to 42.25×10^{10}	10.5×10^{10} to 40×10^{10}	36×10^{10} to 66×10^{10}	105×10^{10} to 200×10^{10}	10×10^{10} to 58.5×10^{10}

The values for asynchronous, DC and air-cooled synchronous machines are similar. Hydrogen or the direct water-cooling method in larger synchronous machines, however, give remarkably higher values.

6.3 Magnetic Loadability

The air-gap flux density and the supply frequency of a machine determine the magnetic loading of the machine. Let us next study how the flux density varies as the speed of a machine increases with increasing line frequency.

Iron losses P_{Fe} are approximately proportional to the square of flux density $\hat{B}_\delta$ and, with high frequencies, to the square of frequency f and to the volume of iron V_{Fe}

$$P_{\mathrm{Fe}} \sim \hat{B}_\delta^2 f^2 V_{\mathrm{Fe}}. \tag{6.33}$$

The maximum rotation speed $n_{\max}$ is proportional to the frequency f, and taking into account Equation (6.24) ($V \sim \lambda^3 \sim n_{\max}^{-3}$), we obtain

$$P_{\mathrm{Fe}} \sim \hat{B}_\delta^2 n_{\max}^2 \frac{1}{n_{\max}^3} = \hat{B}_\delta^2 \frac{1}{n_{\max}}. \tag{6.34}$$

The temperature rise of a machine depends on the power loss per cooling area S. Assuming a constant temperature rise and taking into account Equation (6.24) ($S \sim \lambda^2 \sim n_{\max}^{-2}$), we obtain

$$\frac{P_{\mathrm{Fe}}}{S} \sim \frac{\hat{B}_{\delta}^{2}}{n_{\max} S} \sim \frac{\hat{B}_{\delta}^{2}}{n_{\max}} n_{\max}^{2} = \hat{B}_{\delta}^{2} n_{\max} = \text{constant}. \tag{6.35}$$

Thus, the air-gap flux density depends on the speed:

$$\hat{B}_{\delta} \sim \frac{1}{\sqrt{n_{\max}}}. \tag{6.36}$$

We now get the maximum available power $P_{\max}$ that can be obtained by increasing the speed of the machine. According to Equations (6.13), (6.30), (3.36) and (6.24),

$$P_{\max} \sim A \hat{B}_{\delta} D^{2} l' n_{\max} \sim \frac{1}{\sqrt{n_{\max}}} \frac{1}{\sqrt{n_{\max}}} \frac{1}{n_{\max}^{2}} \frac{1}{n_{\max}} n_{\max} = \frac{1}{n_{\max}^{3}}. \tag{6.37}$$

The power limit is inversely proportional to the cube of the speed. Figure 6.4 illustrates a study of different types of air-cooled machines and shows the rated power that can be reached at a required maximum speed or the maximum speed allowed for a given rated power. The lines in Figure 6.4 are based on conventional electrical and magnetic loading. The figure gives the average values for a large number of machines. Line e represents the limiting power of induction motors, the rotors of which are constructed of smooth solid-steel cylinders, which

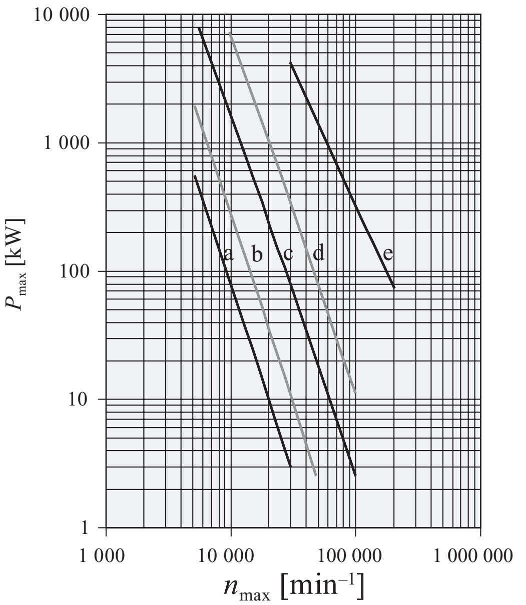

Figure 6.4 Maximum power and speed of air-cooled machines. (a) DC machines, rotor surface speed ≤110 m/s, (b) synchronous cylindrical-rotor machines with a laminated rotor, rotor surface speed ≤130 m/s, (c) induction motors with a laminated squirrel cage rotor, rotor surface speed ≤200 m/s, (d) machines with a solid rotor, rotor surface speed ≤ 400 m/s, (e) induction motors with a solid, copper-coated rotor, rotor surface speed ≤ 550 m/s (a–d: Gutt, 1988; e: Saari, 1998)

are coated with copper cylinders. The cylinder is fixed on the rotor core by explosion welding, which guarantees a perfect mechanical joint between copper and steel.

The limitations of materials decide the realistic upper limits for the power outputs of electrical machines. Present developments in large synchronous machines have led to notable outputs. Today, up to 1500 MW, 1500 min^{-1} synchronous machines are designed as generators of large nuclear power plants. For instance, the rotor dimensions of the nonsalient-pole synchronous generator in the new Finnish Olkiluoto 1793 MW nuclear power plant are $D_r = 1.9\,\mathrm{m}$, $l_r = 7.8\,\mathrm{m}$.

The length of the rotor is chiefly restricted by the critical angular speeds of the rotor. At a critical speed, the rotor has one of its mechanical resonances. There are several bending modes for the mechanics of each rotor. At the lowest critical speed, the rotor bends like a banana having two nodal points. At the second critical speed, the rotor bends into an S-shape with three nodal points, and so on. There are also torsional bending modes that may restrict the use of a rotor. Usually, the ratio of the length of the machine to the air-gap diameter $\chi = l/D$ is selected for operation of the rotor below the first critical rotation speed. This cannot, however, be guaranteed. For instance, large turbogenerators generally operate between different critical speeds. The maximum length of the rotor l_{max} that guarantees operation below the first critical speed is defined according to Wiart (1982)

$$l_{max}^2 = n^2 \frac{\pi^2}{k\Omega}\sqrt{\frac{EI}{\rho S}}, \tag{6.38}$$

where

S is the area of the cross-section of the cylinder (m^2),
E is the modulus of elasticity (Young's modulus) of the rotor material, typically 190–210 GPa for steel,
I is the second moment of inertia of area (m^4), $I = \pi\left(D_{out}^4 - D_{in}^4\right)/64$ for a cylinder,
n is the order of the critical rotation speed,
k is the safety factor (the ratio of the nth critical angular speed to rated angular speed),
ρ is the density of material.

Example 6.5: Calculate the maximum length with a safety factor $k = 1.5$ for a smooth solid-steel rotor operating under the first critical speed, when the rotor diameter is 0.15 m and the rotor speed is 20 000 min^{-1}.

Solution:

$$l_{max}^2 = n^2 \frac{\pi^2}{k\Omega}\sqrt{\frac{EI}{\rho S}}$$

$$l_{max} = \sqrt{1^2 \frac{\pi^2}{1.5\dfrac{20\,000}{60\,\mathrm{s}}2\pi}\sqrt{\frac{200\,\mathrm{GPa}\cdot\dfrac{\pi\cdot 0.15^4}{64}\mathrm{m}^4}{8760\dfrac{\mathrm{kg}}{\mathrm{m}^3}\dfrac{\pi\cdot 0.15^2}{4}\mathrm{m}^2}}} = 0.75\,\mathrm{m}.$$

In this theoretical case $l_{max}/r_r = 10$. In practice, the rotors have slits and low-diameter shafts for bearings and so on, which reduces the l_{max}/r_r ratio.

Table 6.5 Typical $\chi = l'/D$ ratios for different electrical machines

Asynchronous machines	Synchronous machines, $p > 1$	Synchronous machines, $p = 1$	DC machines
$\chi \approx \frac{\pi}{2p}\sqrt[3]{p}$	$\chi \approx \frac{\pi}{4p}\sqrt{p}$	$\chi = 1 - 3$	$\chi \approx \frac{0.8 - 1.6}{p}$

If we employ the safety factor in the yield k_σ, we obtain for the ratio of the length of the rotor to the radius, using Equations (6.23) and (6.38),

$$\frac{l_{\max}}{r_{\mathrm{r}}} = n\pi\sqrt{\frac{k_\sigma}{k}}\sqrt[4]{\frac{C'E}{4\sigma_{\mathrm{mec}}}}. \tag{6.39}$$

This equation yields the maximum length of the rotor after the permitted rotor radius has been defined with Equation (6.23). $l_{\max}/r_{\mathrm{r}}$ is not a function of rotation speed. If a solid-steel rotor rotates below the first critical rotation speed, the ratio should usually be $l/r_{\mathrm{r}} < 7$. In practice, the ratio is often $l/r_{\mathrm{r}} \approx 5$. In the above-mentioned Olkiluoto generator $l/r_{\mathrm{r}} \approx 8.2$.

In standard machines, the ratio of the equivalent machine length to the air-gap diameter

$$\chi = \frac{l'}{D} \tag{6.40}$$

varies within rather tight limits (see Table 6.5).

6.4 Air Gap

The length of the air gap of a machine has a significant influence on the characteristics of an electrical machine. In machines in which the magnetizing current is taken from the supply network, the length of the air gap is dimensioned to produce a minimum magnetizing current and, on the other hand, an optimal efficiency. In principle, a small air gap gives a low magnetizing current, while the eddy current losses of the rotor and stator surface increase because of permeance harmonics created by the open or semi-closed slots. A small air gap also increases the surface losses in the rotor caused by the current linkage harmonics of the stator. Although the air gap is of great significance, no theoretical optimum has been solved for its length, but usually empirical equations are employed instead in the definition of the length of the air gap. An air gap δ of a 50 Hz asynchronous machine can be calculated in metres as a function of power P with the equations

$$\delta = \frac{0.2 + 0.01 \cdot P^{0.4}}{1000}\ \mathrm{m}, \quad \text{when } p = 1, \tag{6.41}$$

$$\delta = \frac{0.18 + 0.006 \cdot P^{0.4}}{1000}\ \mathrm{m}, \quad \text{when } p > 1. \tag{6.42}$$

P must be in watts. The smallest technically possible air gap is approximately 0.2 mm. In drives for extremely heavy duty, the air gap is increased by 60%. In machines with an exceptionally large diameter, an air-gap ratio of $\delta/D \approx 0.001$ has to be selected because of the mechanical properties of the frame and the shaft of the machine.

In frequency converter drives, the air gap may be increased similarly as in heavy-duty drives (60% increase) to get lower rotor surface losses. In large machines with prefabricated windings and open slots, the air-gap length must be selected high enough (60–100% increase) to reduce pulsation losses.

Example 6.6: What is a suitable air gap for a 110 kW, six-pole, heavy-duty induction motor?

Solution:

$$\delta = 1.6\frac{0.18 + 0.006 \cdot P^{0.4}}{1000}\,\mathrm{m} = 1.6 \cdot \frac{0.18 + 0.006 \times 110\,000^{0.4}}{1000}\,\mathrm{m} = 1.285 \times 10^{-3}\,\mathrm{m}.$$

If an asynchronous machine is designed for high speeds, to avoid excessive iron losses in the stator and rotor teeth, the air-gap length has to be increased considerably from the value obtained with Equation (6.41) or (6.42) for a standard electric motor. Also, frequency converter motors may have a larger air gap than motors started direct on line. If a high-speed machine is equipped with a solid rotor, the air gap has to be designed with special care, since the losses at the surface of a solid rotor decrease radically when the air gap is increased, whereas an increase in the magnetizing current in the stator leads to a notably smaller increase in the losses. A suitable value for the length of the air gap has thus to be determined individually in each case.

In DC and synchronous machines, the air gap is basically defined by the permitted armature reaction. We have to ensure that the armature reaction (flux caused by the current linkage of the armature) does not reduce the flux density excessively on one side of a magnetic pole. To meet this condition, the current linkage of the field winding has to be higher than the current linkage of the armature

$$\Theta_\mathrm{f} \geq \Theta_\mathrm{a}. \tag{6.43}$$

This condition may be rewritten for DC machines as

$$\frac{B_{\delta\,\max}}{\mu_0}\delta k_\mathrm{C} \geq \frac{1}{2}\alpha_\mathrm{DC}\tau_\mathrm{p}A_\mathrm{a}. \tag{6.44}$$

On the left of (6.44), we have the field winding current linkage expressed with the no-load air-gap flux density, and, on the right, the armature current linkage expressed by the armature linear current density A_a and the relative pole width α_DC.

Table 6.6 Coefficient γ for the definition of the air gap of DC and synchronous machines

Salient-pole constant air-gap synchronous machines	$\gamma = 7.0 \times 10^{-7}$
Salient-pole synchronous machines, the air gap of which is shaped to produce a sinusoidal flux density distribution	$\gamma = 4.0 \times 10^{-7}$
Nonsalient-pole synchronous machines	$\gamma = 3.0 \times 10^{-7}$
DC machines without compensating winding	$\gamma = 3.6 \times 10^{-7}$
DC machines without compensating winding and commutating poles	$\gamma = 5.0 \times 10^{-7}$
Compensated DC machines	$\gamma = 2.2 \times 10^{-7}$

The same condition for a synchronous machine is given as

$$\frac{\hat{B}_\delta}{\mu_0}\delta k_C \geq \frac{1}{2}\alpha_{SM}\tau_p A_a. \tag{6.45}$$

Then, the air gap of a DC machine must be

$$\delta \geq \frac{1}{2}\alpha_{DC}\mu_0\tau_p\frac{A_a}{B_{\delta\,max}} = \gamma\tau_p\frac{A_a}{B_{\delta\,max}}, \tag{6.46}$$

and for synchronous machines

$$\delta \geq \frac{1}{2}\alpha_{SM}\mu_0\tau_p\frac{A_a}{\hat{B}_\delta} = \gamma\tau_p\frac{A_a}{\hat{B}_\delta}, \tag{6.47}$$

where γ (Table 6.6) includes, according the type of the machine, the relative pole width of the pole shoe α_{DC} or α_{SM}, μ_0 and a constant 1/2.

Example 6.7: A salient-pole synchronous machine with a no-load sinusoidal air-gap flux density has a stator linear current density of $A = 60$ kA/m, an air-gap flux density amplitude of 1 T and a pole pitch of 0.5 m. Find a suitable air gap for the machine.

Solution: The sinusoidal no-load air-gap flux density of the machine results from a suitable pole shape that produces the sinusoidal flux density. Hence, $\gamma = 4 \times 10^{-7}$ and we get

$$\delta_0 = \gamma\tau_p\frac{A}{\hat{B}_\delta} = 4 \times 10^{-7} \cdot 0.5 \cdot \frac{60\,000}{1} = 0.012\,\mathrm{m}.$$

Synchronous reluctance machines must have a high inductance ratio, which suggests selecting a small d-axis air gap. To be able to compete with the performance of asynchronous machines, synchronous reluctance motors may have to be equipped with smaller d-axis air gaps than those in induction motors. However, if the air gap is made very small, the surface loss, because of permeance harmonics, may increase remarkably if high-quality rotor laminations are not used.

In doubly salient reluctance machines, the aim is to construct as small an air gap as possible to achieve a high inductance ratio between the direct and quadrature position of the machine.

In PMSMs, the air-gap length is determined by mechanical constraints. It is similar to those values encountered in asynchronous machines and can be calculated from Equations (6.41) and (6.42). The synchronous inductance depends on the air-gap length. Since the magnet length itself has a significant influence on the magnetic air gap of the machine, the synchronous inductance easily becomes low and the machine maximum torque high. However, in some cases, the thickness of the magnet and even the length of the physical air gap must be increased to get a smaller synchronous inductance. Generally, the physical air gap is made as small as possible to save the amount of material in the permanent magnet. This holds especially for low-speed, high-torque permanent magnet machines. In higher-speed machines, the air-gap harmonic content may cause very high losses in the permanent magnet material or in the ferromagnetic material under the permanent magnets, and in such cases the air gap must be increased to keep the magnet temperature low enough. In a PMSM, the determination of the air gap and the thickness of the magnets themselves is thus a demanding optimization task.

In rotor surface magnet machines, the magnetic air gap of the machine may be calculated as

$$\delta_{\mathrm{PM}} = h_{\mathrm{PM}}/\mu_{\mathrm{rPM}} + \delta_{\mathrm{e}} \tag{6.48}$$

where h_{PM} is the rotor surface permanent magnet thickness, μ_{rPM} the permanent magnet material relative permeability and δ_{e} the equivalent air gap, the physical air gap corrected with the Carter factor ($\delta_{\mathrm{e}} = k_{\mathrm{C}}\delta$).

If the magnets are embedded, their effects in the reluctance of the magnetic circuit are somewhat complicated and have to be taken into account in the calculation of the effective air gap δ_{ef}. Numerical methods are often applied.

Bibliography

Gutt, H.-J. (1988) Development of small very high speed AC drives and considerations about their upper speed/output limits. *Proceedings of Conference on High Speed Technology, August 21–24, 1988. Lappeenranta, Finland,* pp. 199–216.

Lawrenson, P.J. (1992) A brief status review of switched reluctance drives. *EPE Journal*, **2** (3), 133–44.

Marchenoir, A. (1983) High speed heavyweights take on turbines. *Electrical Review*, **212** (4), 31–3.

Miller, T.J.E. (1993) *Switched Reluctance Motors and Their Controls*, Magna Physics Publishing and Clarendon Press, Hillsboro, OH and Oxford.

Richter, R. (1954) *Electrical Machines: Induction Machines (Elektrische Maschinen: Die Induktionsmaschinen)*, Vol. **IV**, 2nd edn, Birkhäuser Verlag, Basle and Stuttgart.

Richter, R. (1963) *Electrical Machines: Synchronous Machines and Rotary Converters (Elektrische Maschinen: Synchronmaschinen und Einankerumformer)*, Vol. **II**, 3rd edn, Birkhäuser Verlag, Basle and Stuttgart.

Richter, R. (1967) *Electrical Machines: General Calculation Elements. DC Machines (Elektrische Maschinen: Allgemeine Berechnungselemente. Die Gleichstrommaschinen)*, Vol. **I**, 3rd edn, Birkhäuser Verlag, Basle and Stuttgart.

Saari, J. (1998) *Thermal Analysis of High-Speed Induction Machines*, Acta Polytechnica Scandinavica, Electrical Engineering Series No. 90. Helsinki University of Technology.

Vogt, K. (1996) *Design of Electrical Machines (Berechnung elektrischer Maschinen)*, Wiley-VCH Verlag GmbH, Weinheim.

Wiart, A. (1982) New high-speed high-power machines with converter power supply, *Motorcon Proceedings, September 1982*, pp. 641–6.